

Cascaded DC–DC Converter Connection of Photovoltaic Modules

Geoffrey R. Walker, *Member, IEEE*, and Paul C. Sernia

Abstract—New residential scale photovoltaic (PV) arrays are commonly connected to the grid by a single dc–ac inverter connected to a series string of pv panels, or many small dc–ac inverters which connect one or two panels directly to the ac grid. This paper proposes an alternative topology of nonisolated per-panel dc–dc converters connected in series to create a high voltage string connected to a simplified dc–ac inverter. This offers the advantages of a “converter-per-panel” approach without the cost or efficiency penalties of individual dc–ac grid connected inverters.

Buck, boost, buck-boost, and Cúk converters are considered as possible dc–dc converters that can be cascaded. Matlab simulations are used to compare the efficiency of each topology as well as evaluating the benefits of increasing cost and complexity. The buck and then boost converters are shown to be the most efficient topologies for a given cost, with the buck best suited for long strings and the boost for short strings. While flexible in voltage ranges, buck-boost, and Cúk converters are always at an efficiency or alternatively cost disadvantage.

Index Terms—Cascaded converter, grid connected photovoltaic (PV), Matlab efficiency simulation, maximum power point tracking (MPPT), module integrated converters (MICs), multilevel converter, series connected converter.

I. INTRODUCTION

WITH AN increasing worldwide interest in sustainable energy production and use, there is renewed focus on the power electronic converter interface for dc energy sources. Three specific examples of such dc energy sources that will have a role in distributed generation and sustainable energy systems are the photovoltaic (PV) panel [1], the fuel cell stack [2], and batteries of various chemistries [3].

II. SERIES CONNECTED PV PANELS

These dc energy sources are all series and parallel connections of a basic “cell.” These cells all operate at a low dc voltage, ranging from less than 1 V (PV cell) to 3 or 4 V (Li–Ion cell). These low voltages do not interface well to existing higher power systems, so the cells are series connected to create a battery, a fuel cell stack, or a PV module or panel with a higher terminal voltage. (The term PV panel rather than PV module will be used in this paper to avoid confusion with the proposed attached power electronic modules.)

For example “12-V” PV panels have 36 solar cells with a maximum power point (MPP) of approximately 16–17 V under standard test conditions. These system voltages are appropriate

for lower power systems, but beyond powers of a few hundred Watts (W), these panels themselves are placed in series strings to maintain lower currents and higher efficiencies. These long strings of panels (and hence cells) bring with them many complications.

PV panels in a string are never exactly identical. Because PV panels in a series string are constrained to all conduct the same current, the least efficient panel, and indeed cell, sets this string current. The overall efficiency of the array is reduced to the efficiency of this cell. This also means that PV panels in a string must be given the same orientation and be of identical size.

A more profound problem occurs when even a single cell in the array is shaded. The photocurrent generated in a shaded cell may drop to perhaps 20% of the other cells. The shaded cell will be reverse biased by the remaining cells in the series string, but current will continue to flow through it causing large localized power dissipation. A diode around a group of 18 cells (half a 12-V panel) limits the reverse bias and hence the power dissipation in the shaded cell. However, all the power from that sub string is lost while current flows in the bypass diode [1].

Placing a dc–dc converter on each half-panel or panel sub-string, and then connecting these *converters* in series strings avoids many of these problems. This paper examines the advantages, difficulties, and implementation issues of using a cascaded converter connection for a series string of PV panels, or more generally dc energy sources. A proposed residential grid connected solar installation consisting of twelve 12-V 60-W PV panels is used where a specific example is helpful in developing the discussion.

III. CONVERTER INTERFACE OF PV PANELS

In grid-connected inverters for PV applications, a number of different approaches have been developed and used over the last 20 years. An excellent review of such systems available in Europe is given in [4]. Only the two more common approaches used in smaller residential scale installations (1–3 kW) are compared here (see Fig. 1).

A. Single DC String, Single DC–AC Inverter

In a residential system of say 2 kW or less, all the PV panels on the rooftop can be connected electrically in series, to create a high voltage low current dc source. This source is connected to a single dc–ac inverter within the roof or house. The ac then runs to the residential switchboard.

B. Individual DC–AC Inverters per Panel (Module Integrated Converters)

In this more recent approach, each PV panel has its own dc–ac inverter, mounted at the panel on the rooftop. A 240-V ac connection from the switchboard runs to the rooftop, and loops from

Manuscript received February 13, 2003; revised September 12, 2003. Recommended by Associate Editor Z. Chen.

The authors are with the School of Information Technology and Electrical Engineering, The University of Queensland, Brisbane 4072, Australia (e-mail: walkerg@itee.uq.edu.au; psernia@itee.uq.edu.au).

Digital Object Identifier 10.1109/TPEL.2004.830090

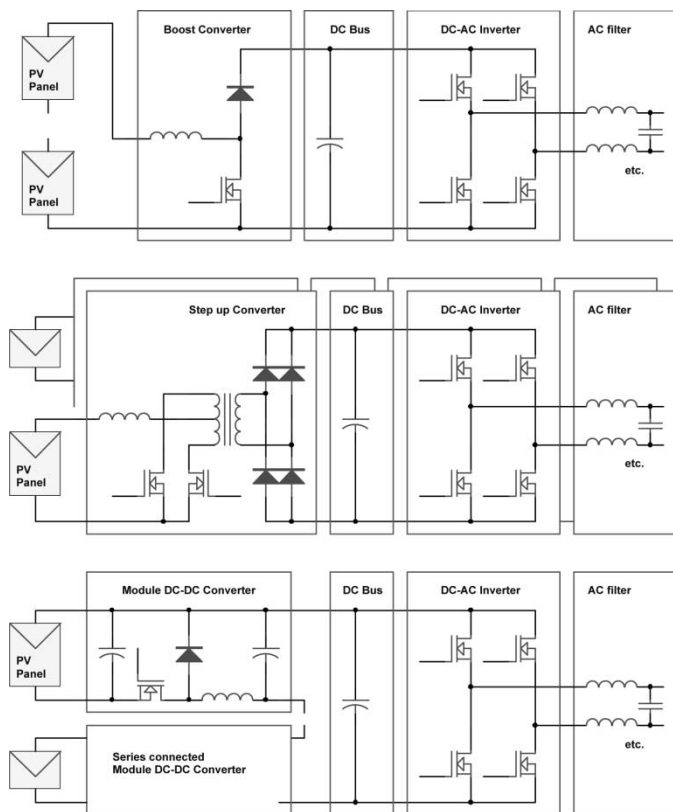


Fig. 1. Comparison of three grid connected PV inverter topologies discussed in the text—a single dc-ac inverter connected to a single dc PV string (top); a module integrated dc-ac inverter for every PV panel (middle); or the proposed series connected panel integrated dc-dc converters connected to a centralised dc-ac inverter (bottom).

inverter to inverter, panel to panel. Each panel is now effectively placed in parallel, via its own dedicated inverter.

To be small, light and low cost, module-integrated converters generally use high frequency switch mode techniques. To efficiently convert the panel's low dc voltage to the 240-V ac grid voltage they invariably require a transformer isolated converter. Most approaches rectify to a high voltage dc bus which is followed by an ac inversion stage and line side filtering.

C. Multi-Converter Strings—Panel Integrated DC-DC, String DC-DC

The approach proposed in this paper combines aspects of these two approaches. Every panel has its own converter, but these converters are dc-dc converters, and the panels with their associated converters are still placed in series to form a dc string. A single dc-ac inverter is then required to connect to the grid. This intermediate solution is argued to combine the best features of the two existing approaches presented.

IV. EXAMINATION OF PROPOSED APPROACH

A. Advantages of a Converter-per-Panel Approach

A panel integrated converter approach whether dc-dc or dc-ac has many advantages. Specific application examples for battery strings as well as PV applications are given to help illustrate each case.

1) *Better Utilization on a per Module Basis:* Each converter module can independently control and so optimize the power flow to or from its source. For a battery string, each converter can independently and optimally charge its connected battery, reducing equalization time and increasing charge efficiency.

In a solar power application, each converter can independently perform maximum power point tracking (MPPT) for its PV panel. In an otherwise ideal installation, this will compensate for mismatches in panels of like manufacture, which can be up to 2.5% [5]. It offers the further advantage of allowing panels to be given different orientations and so open up new possibilities in architectural applications. A third advantage is the greater tolerance to localized shading of panels. These reasons taken together are the most important advantage of per-panel distributed converters in PV applications.

2) *Mixing of Different Sources Becomes Possible:* Independent and intelligent power flow control can decouple each source from the others in the string. Batteries could be replaced individually as required since old and new batteries can now be mixed. Existing PV panel strings could be extended by adding new higher output panels without compromising overall string reliability or performance.

3) *Better Protection of Power Sources:* Intelligent protection can be applied on a per source basis. For example, a weak battery can be protected from permanent damage during deep discharge. A single shaded PV panel can deliver its reduced power rather than being bypassed by a diode for its own protection.

4) *Redundancy of Both Power Converters and Power Sources:* An intelligent converter module can bypass a failed source or indeed a failed converter if appropriately designed, allowing the complete installation to continue operation at slightly reduced capacity.

5) *Better Data Gathering:* Each power source/power converter module will have an inherent data collection capability and most likely a control network connection, so that data gathering and reporting will add minimal additional complexity or cost. Batteries or PV panels requiring inspection or replacement can be individually identified.

6) *Greater Safety During Installation and Maintenance:* Depending on design, each converter module may be able to isolate its connected power source, so that the wiring of series or parallel connections of these modules can be performed safely. The power source—converter connection is a safe low voltage connection.

7) *Cost Justification or Advantage:* In most applications, many small converter modules, one per source, will displace one large converter. The total VA (power) rating of the power switching devices will remain the same, but the cost of the distributed solution could be more attractive in time because

- 1) the hardware functionality of the modules could be standardised. They could be made in significant volumes by a number of manufacturers. They could be integrated, packaged and sold with the dc source. They could be adapted to different applications through software updates;
- 2) the advantages of greater efficiency and reliability would increase the return on the installation investment;
- 3) the advantages of per module data acquisition, intelligent protection and control could displace additional hardware that might otherwise be required.

B. Series Versus Parallel String of Module Integrated Converters

The present grid connected module integrated converters that convert directly to 240-V ac can lay claim to most of these advantages. However, this approach of direct grid connection has the disadvantage of a large difference between the converter input voltage (low) and output voltage (high). This requires a transformer based converter, which requires more mass and volume, is more expensive and is less efficient than a simple nonisolated dc–dc converter.

A series rather than parallel connection of converters allows the input-output voltage ratio to be close to unity, which leads to the highest switch utilization and removes the need for a transformer. Efficiencies of close to 100% are possible and converters can be small, light and low cost.

A series connection utilizes low voltage MOSFETs, Schottky diodes, inductors and capacitors that have been developed for low voltage dc–dc converters. A parallel connected converter requires high voltage fast recovery diodes and MOSFETs, which are at a performance versus cost disadvantage.

C. Why Not per Panel DC–AC Cascaded Converters?

One converter structure—the cascaded full bridge [6], [7]—could also be distributed on a per panel basis operating at low voltage, with a series connection of converters to achieve direct (transformer-less) 240-V ac grid connection. This would maintain the above stated benefits, and further remove the need for the per-string dc bus and dc–ac inverter. This structure is promising and deserves further consideration and research, however it is not pursued further here for the following reasons.

- 1) AC grid connection details such as filtering, protection, and control including anti-islanding must all be distributed to the per-panel converters.
- 2) The energy storage capability required for single phase ac connection of converters must be distributed to the per-panel converters. This generally requires electrolytic capacitors in the harsh PV panel environment.
- 3) Issues of electromagnetic interference may become more complex in a distributed ac implementation.

D. Previous Series Connected DC–DC Converter Research

While there are many examples of series connected dc–ac converters, otherwise known as cascaded full-bridge converters, as discussed in the previous section, there is little relevant work on series connected dc–dc converters which was discovered by the author.

Enslin *et al.* [8] present “A low-power low-cost highly efficient maximum power point tracker (MPPT) [designed] to be integrated into a photovoltaic (PV) panel.” The resonant switching buck converter with a synchronous rectifier achieves better than 98% efficiency for much of its operating region. Its simple analog implemented MPPT algorithm is reported to allow the dc–dc converter modules to be placed in series and operate correctly with no inter-module communication, although no detailed analysis of such a series connection is presented.

The control of modular dc–dc converters with series input and parallel output connections is examined by Giri *et al.* [9]. They show a common converter control signal is all that is required to ensure input voltage and output current sharing. The converters

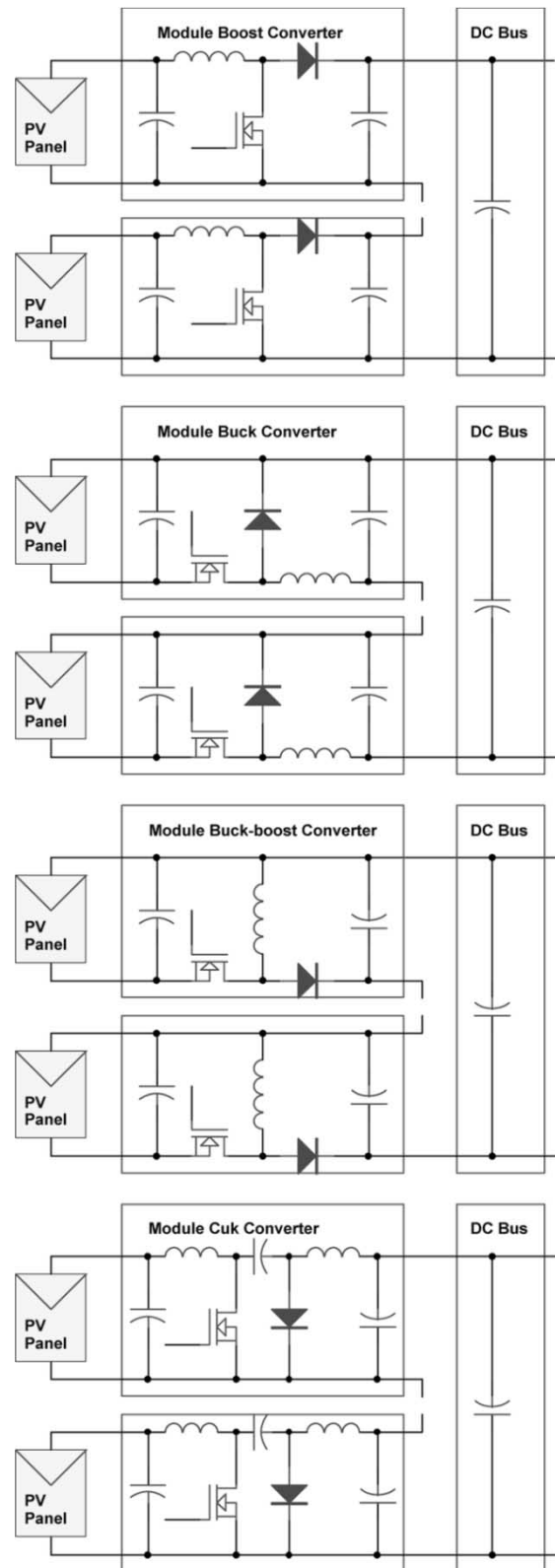


Fig. 2. Four possible nonisolated dc–dc converter topologies considered—Boost, Buck, Buck-boost, and Cuk. Each is shown with an N-channel MOSFET connected for low-side drive relative to the PV panel. Note that the output voltage is inverted for the two inverting converters (buck-boost and Cuk). Only two of many series modules are shown in each string.

considered are buck derived and isolated by necessity of the common input and output connections.

V. SUITABLE DC-DC CONVERTERS

Four possible nonisolated dc-dc converter topologies are considered in turn for their suitability as PV panel converters (Fig. 2)—the boost, buck, buck-boost and Cúk. Each is shown with an N -channel MOSFET configured as a low side switch relative to the dc source, the PV panel. If bidirectional power flow is desired for sources such as batteries, then the diode must be replaced with a second MOSFET to create a half-bridge.

A. Boost Converter Modules

A boost converter initially appears the most promising candidate for a series connected integrated dc-dc converter. A boost characteristic allows the required 340-V minimum dc bus voltage (for 240-V transformer-less ac grid connection) to be achieved with fewer PV panels. With the open circuit voltage of the PV panel set below the desired converter output voltage, a boost characteristic would also allow the maximum power point (MPP) to always be tracked [10].

The output current in a series string of converters must be equal, so the output voltages of the converters are proportional to the power each converter is delivering. An additional constraint for boost converters is $V_{IN} \leq V_{OUT}$ and $I_{IN} \geq I_{OUT}$. Should one PV panel be shaded, its current will fall, and if this value is lower than the string output current, then the current in the entire string must fall to the value of the lowest converter module input current. In practice, a better control strategy may be to force the input and output voltage of that one converter module to zero under these circumstances, at which point that module can pass the required output current via its semiconductor switches. Note that while this operating regime may allow the remaining panels to operate at or near their MPPs, the shaded PV panel is short-circuited. While simply undesirable for PV panels, this would be an unacceptable situation for batteries or fuel cell sources!

This situation only occurs for significant mismatches in power outputs if a significant voltage boost is being used. Consider a system of twelve 60-W rated PV panels each delivering 15 V and 3 A (see Fig. 3). A boost converter on each panel operates at 50% duty in continuous conduction mode (CCM) to boost the output voltages to 30 V at 1.5 A for a combined series total of 360 V and 540 W. One panel must drop to slightly less than 1.5 A (1.44 A) or 20 W before other panels are forced away from their MPPs.

Below a string current of 1.38 A, the power forfeited in the remaining eleven panels exceeds the power gained by continuing to include the underperforming panel. In this case, this panel should be short circuited, forfeiting its power, but allowing the remaining panels to deliver their maximum power of 495 W. When several panels are affected by different degrees of shading, this clearly becomes a difficult control problem.

The inductor on the PV panel side will reduce the EMI and losses due to ripple in the converter. The ripple on the output capacitor side can be partially cancelled by the application of multilevel switching techniques [11].

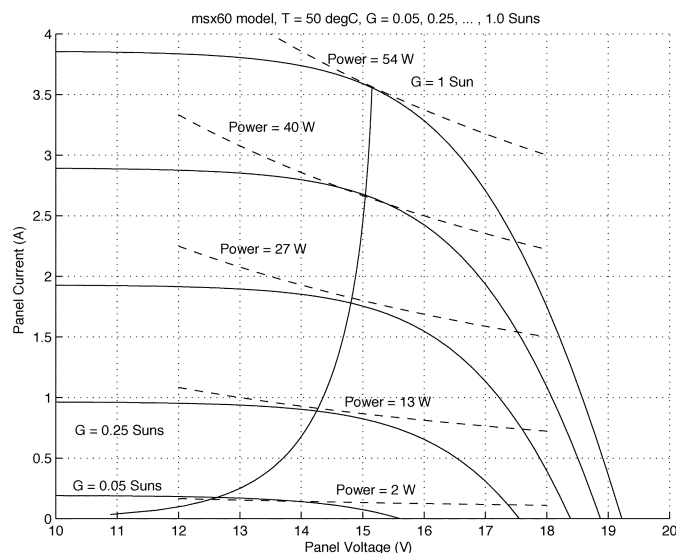


Fig. 3. Locus of the maximum power point (MPP) for varying power levels at a constant cell temperature of 50 °C for the MSX60 60-W panel [10], [13]. In practice, as illumination and power falls, the cell temperature will drop from this elevated temperature back to ambient, causing the open circuit and MPP voltage to rise. It is fair to assume a reasonably constant MPP voltage of 15 V.

B. Buck Converter Modules

In a buck converter, the output voltage must always be less than the input voltage. Assuming a goal of tracking the MPP down to a minimum PV panel output voltage of 12 V (1 W from 60-W panel, at 50 °C, as shown on Fig. 3) [10], a minimum of thirty series PV panels and converters are required for a 360-V dc bus.

More panels still are required to allow for significant shading, or bypassing failed panels. For example, if seven of the 30 panels are shaded to the point where their power output drops to 7 W, then the remaining panels need to generate 15 V at 3 A to ensure 360 V can be generated.

In their favor, a series string connection of buck modules does allow total independence of output voltage and hence power, while the output currents are forced equal by the series connection. Further, the internal freewheel diode allows an inactive or failed module to automatically be bypassed without shorting the dc source.

The input filter capacitor must be sized to handle the switching ripple current of the buck converter. The output filter inductor and capacitor could be chosen based on a multilevel converter design strategy to achieve significant component size reductions.

C. Buck-Boost or Cúk Converter

The buck-boost and Cúk inverting converters are traditionally not favored because of their poor switch utilization, achieving a maximum of 25% at a duty ratio of 50%, when $V_{IN} = V_{OUT}$ [for continuous conduction mode (CCM)] [12]. This however is not a particularly significant issue at the low PV panel voltages of 21 V maximum, and powers of less than 100 W considered here. It will however mean that these converters are unlikely to achieve the same efficiency as the buck or boost converters.

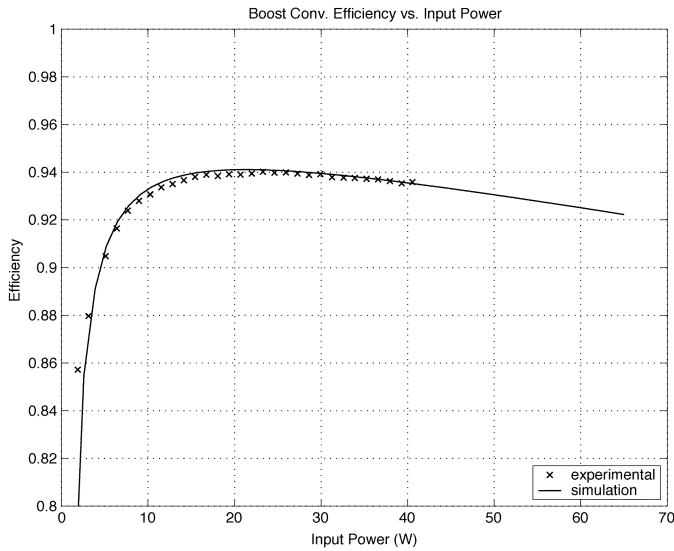


Fig. 4. Experimentally measured and theoretically calculated efficiency of the 15 to 30-V boost converter configuration.

The buck-boost converter has discontinuous and thus high input and output capacitor ripple, which requires large capacitor ripple current ratings, and can introduce significant noise problems. The Cúk converter has low input and output current ripple and noise, but at the expense of extra circuit complexity and cost.

These converters do have the advantage of being able to generate output voltages both above and below the input voltage. The nominal duty ratio is thus best set at 50% where they achieve their best switch utilization and greatest efficiency. For a 360-V dc bus and a 15-V MPP, 24 panels would be optimal. Any number of panels from 12 to 36 equating to converter output voltages of 30 to 10 V would still lead to a reasonable converter specification for design.

Both these converter topologies allow individual module outputs to fall to zero while allowing other modules to continue to operate their panels at their maximum power point.

VI. EXAMPLE CONVERTER DESIGNS

To best assess the relative merits of the converters presented, a design for a string of MSX60 60-W PV panels connected to a 360 V regulated dc bus is considered. The choice of 360 V is based on an ac mains voltage of 230 V +10%, or 240 V +6%.

The Solarex MSX60 panel (now called the BPsolar BP SX 60) [10], [13] is a representative mid sized panel, with the following specifications relevant to this work:

Max Voltage	23 V at 0 A, 1 Sun, 0 °C;
Max Current	5 A at 0 V, 1.3 Sun, 50 °C;
Exp. Max MPP	15 V * 5 A = 75 W at 1.3 Sun, 50 °C;
Exp. Min MPP	12 V * 0.2 A = 2.5 W at 0.05 Sun, 50 °C.

Four different series connected module per-panel dc-dc converter designs will be considered: a boost, a buck, a buck-boost, and a Cúk.

A. Matlab Simulation of Converter Losses

A Matlab script file was written to calculate the losses and thus efficiency of these various topologies from first principles.

Using this method, the effect on loss of varying certain parameters such as switching frequency was quickly evident. It also made it easy to see the relative magnitude of the various losses.

The first step in calculating the losses was to calculate the RMS currents in the various components of the circuit. For example, in the boost converter, the peak to peak inductor ripple current i_L (1) along with the average inductor current which is the input current I_i is used to calculate the RMS inductor current (3). From this the RMS switch current $I_{Q,RMS}$ (4) and RMS diode current $I_{D,RMS}$ (5) can be calculated given the respective duty cycles D and $(1 - D)$ of these devices. The input and output capacitor RMS currents $I_{C_i,RMS}$ (6) and $I_{C_o,RMS}$ (7) are the ac components of the input and output currents. For simplicity, these formulae all assume continuous conduction mode (CCM), which was true in this study to approximately 10% of the converters rated current. The minimum inductor current (2) is calculated to check for the boundary of CCM

$$i_L = t_{on} * \frac{V_i}{L} \quad (1)$$

$$I_{L,min} = I_i - \frac{i_L}{2} \quad (2)$$

$$I_{L,RMS} = \sqrt{I_i^2 + \frac{i_L^2}{12}} \quad (3)$$

$$I_{Q,RMS} = \sqrt{I_{L,RMS}^2 * D} \quad (4)$$

$$I_{D,RMS} = \sqrt{I_{L,RMS}^2 * (1 - D)} \quad (5)$$

$$I_{C_i,RMS} = \frac{i_L}{\sqrt{12}} \quad (6)$$

$$I_{C_o,RMS} = \sqrt{I_{D,RMS}^2 - I_o^2}. \quad (7)$$

With these RMS currents calculated, the conduction (I^2R) losses of the inductor P_L (8), MOSFET switch $P_{Q,c}$ (9), input capacitor P_{C_i} (14) and output capacitor P_{C_o} (15) are easily modeled. The MOSFET switching losses $P_{Q,s}$ (10) assume a linear rise in current and then fall in voltage during the turn on period $t_{sw,on}$ and vice versa during the turn off period $t_{sw,off}$. The MOSFET gate drive losses $P_{Q,g}$ (11) are calculated by noting that during each switching cycle the MOSFET gate is charged to the MOSFET gate drive supply V_{gg} and then discharged to ground. This represents an average current of $Q_g * f$ flowing from the gate drive supply V_{gg} . The forward voltage drop of the diode was initially modeled as a constant forward drop and an incremental resistance, however it was found that a forward drop V_{fwd} alone provided sufficient accuracy in the calculation of the diode conduction losses P_D (12). Since a Schottky diode was used, diode switching losses were assumed to be zero. Finally a constant additional power loss P_{misc} was added to account for other unaccounted losses such as inductor core losses.

No power was allocated to control, since modern microcontrollers are available which can operate with less than 1 mW of power. The Texas Instruments MSP430 series 16-bit RISC microcontrollers for example feature the necessary analog to digital converters, timers and serial communications peripherals and operate at 250 μ A/MIP. Similarly op-amps, communica-

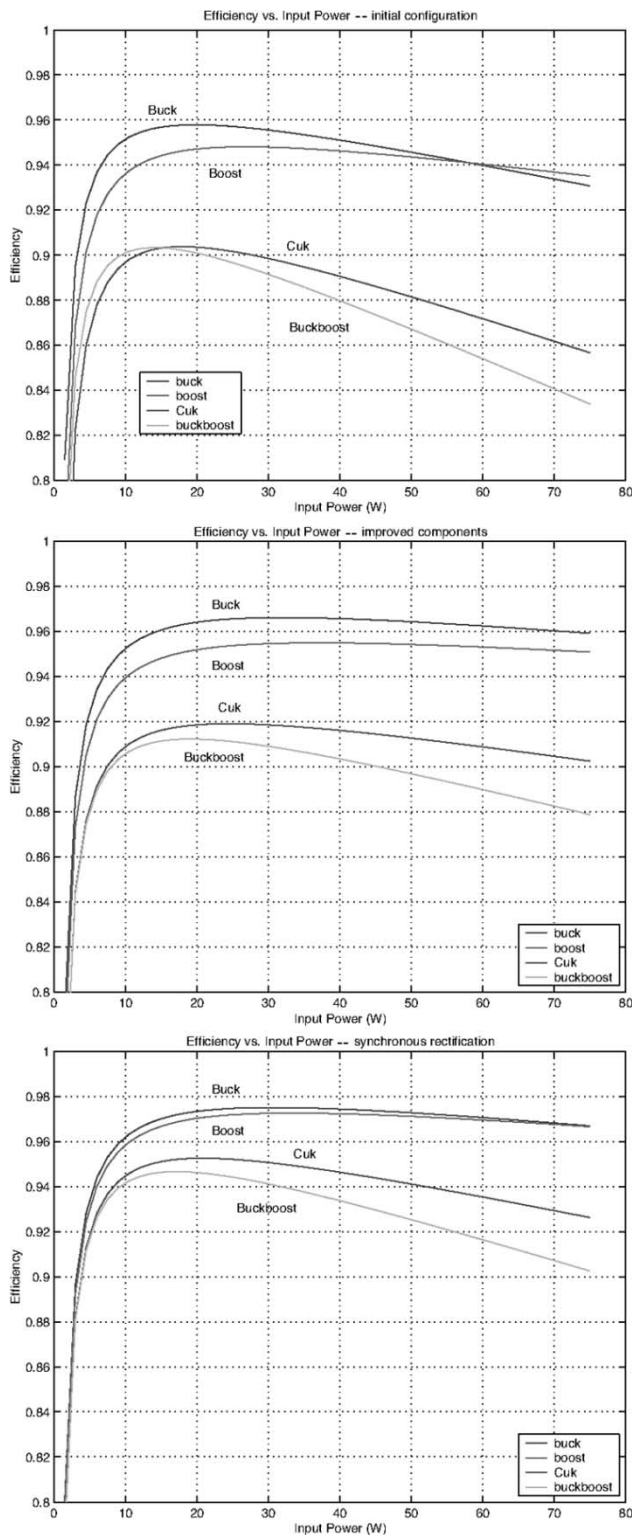


Fig. 5. Theoretically calculated efficiencies of four dc-dc converter configurations—buck, boost, buck boost, and Cúk. The top plot is for the original specification of converter, while the middle and bottom plots show the improvements due to lower resistance MOSFETs and inductors (middle), and then additionally, the use of MOSFETs as synchronous rectifiers in place of Schottky diodes (bottom).

tions transceivers and gate driver ICs are all available with very low operating currents

$$P_L = I_{L,RMS}^2 * R_L \quad (8)$$

$$P_{Q,c} = I_{Q,RMS}^2 * R_{DSon} \quad (9)$$

$$P_{Q,s} = 0.5 * I_i * V_o * f * (t_{sw,on} + t_{sw,off}) \quad (10)$$

$$P_{Q,g} = Q_g * V_{gg} * f \quad (11)$$

$$P_D = V_{fwd} * I_i * (1 - D) \quad (12)$$

$$P_{C_i} = I_{C_i,RMS}^2 * R_{C_i} \quad (13)$$

$$P_{C_o} = I_{C_o,RMS}^2 * R_{C_o} \quad (14)$$

$$P_{misc} = \text{constant.} \quad (15)$$

The Matlab script file which implements these equations to calculate the power losses and efficiency of a boost converter is listed in Appendix A.

B. Boost Converter Experimental Validation of Matlab Simulation

To validate the efficacy of the Matlab model developed, a test case of an example boost converter was completed first. After specifying the design, it was both modeled in Matlab and built and tested experimentally.

A 360-V string of twelve series connected boost converters leads to a 30-V converter output voltage, so $P_{IN} = 15 \text{ V} * 5 \text{ A}$, $P_{OUT} = 30 \text{ V} * 2.5 \text{ A}$. A first attempt is a simple low cost design using a low side *N*-channel MOSFET, a Schottky diode, low ESR capacitors and a prewound inductor. The components chosen are in the first section of the table at the bottom of the next page.

The switching frequency chosen was 100 kHz, which leads to an input current ripple of 0.75 A in a 100- μH inductor. A higher switch frequency begins to lead to excessive switching losses, a lower value requires a larger *LC* filter with higher associated parasitic losses. The Schottky diode avoids reverse recovery issues and associated losses at high frequencies, so CCM is preferred to lower other losses. The capacitors are sized based on their ripple current ratings.

Once this converter was built, its input and output voltages and currents were measured at a number of power levels and switching frequencies. From these a number of loss versus power, and efficiency versus power curves were created at different frequencies. These were used to experimentally confirm and then fine-tune the Matlab converter model that calculated loss and efficiency from first principles (see Appendix A for the example Matlab script file).

Fig. 4 shows the correspondence of this Matlab model to the experimentally gathered results. The efficiency of this converter was not especially good, ranging from 92–94% from 10–60 W. A loss of 8% or 5 W in 60 W is very significant when the source of those Watts are expensive PV panels.

Note that the simulation generally assumed the 25 °C values for resistances and voltage drops and likewise the experimental work was also carried out in a laboratory at room temperature. This was done for a number of reasons—it was difficult to get consistent datasheet information at temperatures other than 25 °C, it would have been more difficult to conduct the experimental work at an artificially elevated temperature, and finally, it is difficult to estimate what the final converter operating temperature would be anyway.

In the final application these converters would most likely be mounted behind the PV panels or possibly in their junction boxes and would operate in an ambient environment of approximately 50 °C. Assuming the power dissipation of the compo-

TABLE I
MATLAB SCRIPT FILE

```

% pppta3_eff1_f100_for_jrnl.m
% calcs power loss and efficiency of boost converter ...
% a) from experimentally gathered data, then
% b) from first principles by summing losses in each component
% based on the component parameters and operating point.
% Then plots experimental and calculated loss and eff. to compare.
% assumes continuous conduction (CCM)
% [1] Fundamentals of power electronics, Robert W. Erickson
% [2] Power Electronics: Converters, applications and design,
%      Mohan, Undeland, Robbins.
% [3] Motorola Datasheet MBR735/D

load ..\data1\eff100k50p26v.txt
iviv = eff100k50p26v;
pin = iviv(:,1) .* iviv(:,2);
pout = iviv(:,3) .* iviv(:,4);
ploss = pin - pout; % experimental data power loss vector
eff_real = pout./pin; % experimental data efficiency vector

Vi = 13; Vo = 26;
Ii = 0.1:0.1:5.0; Pones = ones(size(Ii));
eff_0 = 0.95; % an initial guess to calc Pout and Io.

Pi = Vi .* Ii; Po = eff_0 * Pi; Io = Po / Vo;

f = 100000; T = 1 / f; D = 1-(Vi/Vo); ton = D * T;
tsw = 150e-9; % t_ri + t_fv + t_rv + t_fc
Qg = 13e-9; Vgg = 5; % total MOSFET gate charge and drive V.

L = 100e-6; RL = 0.046; % L's Inductance and winding resistance
Rs = 0.07; % Ron of MOSFET (IRFZ24)
% Tried simple straight line approx forward voltage drop
% of Schottky MBR745 at 75 degC [3] -> Vf = 0.33 + 0.05.*Ii;
% However found schottky is best modelled as const drop, since
% rising current (rising Vf) is matched by rising temp (falling Vf)
Vf = 0.43; % Vf of Schottky (MBR745)
Rcin = 0.87; Rcout = 0.10; % ESR of Cin and Cout respectively
Pl_misc = 0.25; % Miscelaneous losses, const vs Pin, eg Fe loss in L.

% The following current calculations all assume CCM
iL = ton*Vi/L; % p-p Inductor current ripple
ILmin = Ii - iL/2; % Min inductor current
ILrms = sqrt(Ii.^2 + iL.^2/12); % RMS inductor current - eqn A1.2 [1]

```

nents themselves is low and adequate heat sinking is provided, their temperatures should certainly remain below 100 °C. A temperature rise of 50 °C will cause the MOSFET on resistance to rise by 35% and the inductor copper resistance by 20%, but the Schottky diode forward voltage drop will fall by 6% and capacitor ESR also falls with increasing temperature.

As a precaution, the simulation was re-run with increased resistances as indicated above. An additional 0.5-W loss at 60-W input power caused a 1% drop in efficiency. The difference was much less at lower powers since the additional losses were I^2R in nature. All subsequent simulations were conducted using 25 °C datasheet values.

TABLE I (CONTINUED)
MATLAB SCRIPT FILE

```

Iqrms = sqrt(ILrms.^2 * D);      % RMS switch current   - eqn A1.6 [1]
Idrms = sqrt(ILrms.^2 * (1-D)); % RMS diode current   - as above
ICi = iL / sqrt(12);           % RMS input cap current - eqn A1.9 [1]
ICo = sqrt(Idrms.^2 - Io.^2);   % RMS output cap current -eqn 3-28 [2]

Pl_L = ILrms.^2 * RL;          % Inductor loss
Pl_Qc = Iqrms.^2 * Rs;         % Switch loss (conduction)
Pl_Qs = 0.5 * Ii * Vo * tsw * f; % Switch loss (switching)
Pl_Qg = Qg * Vgg * f .* Pones; % Switch loss (gate drive)
Pl_D = Vf .* Ii * (1-D);      % Diode loss
Pl_Ci = ICi.^2 * Rcin .* Pones; % Cin loss
Pl_Co = ICo.^2 * Rcout;       % Cout loss
Pl_misc = Pl_misc .* Pones;   % miscellaneous const loss

Pl = [ Pl_D; Pl_L; Pl_Qc; Pl_Qs; Pl_Co; Pl_misc; Pl_Ci; Pl_Qg ];
Pl_tot = sum(Pl);              % Total Power loss
eff = (Pi - Pl_tot)./Pi;

% Calculated component losses for relative comparison
figure(1); plot(Ii,Pl); grid on;
Title('Boost conv. Losses vs. Input Current');
xlabel('Input current (A)'); ylabel('Power losses (W)');
legend('Pl_D - Diode conduction',...
      'Pl_L - Inductor ESR',...
      'Pl_{Qc} - MOSFET conduction',...
      'Pl_{Qs} - MOSFET switching',...
      'Pl_{Co} - output cap ESR',...
      'Pl_{misc} - misc const loss',...
      'Pl_{Ci} - input cap ESR',...
      'Pl_{Qg} - MOSFET gate drive',2);

figure(2); % Experimental & calced efficiency vs. P_in
plot(pin,eff_real,'x',Pi,eff,'-'); grid on;
Title('Boost Conv. Efficiency vs. Input Power');
xlabel('Input Power (W)'); ylabel('Efficiency');
legend('experimental','simulation',4);
ax = axis; ax(1,3) = 0.8; ax(1,4) = 1.0; axis(ax);

figure(3); % Experimental & calced losses vs. P_in
plot(pin,ploss,'x',Pi,Pl_tot,'-'); grid on;
Title('Boost Conv. Losses vs. Input Power');
xlabel('Input Power (W)'); ylabel('Losses (W)');
legend('experimental','simulation',2);
ax = axis; ax(1,4) = 5; axis(ax);

```

C. Comparison of Converters

Having gained some confidence in the accuracy of the Matlab model of the boost converter, the losses of all four converters

considered in this paper were modeled in Matlab using a similar selection of components. Two 2200- μF capacitors were used where discontinuous current was expected; one 220- μF capacitor where an inductor made the current continuous.

MOSFET	IR IRFZ24N	55 V, 18 A, 70 m Ω
Schottky Diode	Motorola MBR745	45 V, 7 A, 0.43 V at 5 A, 125 °C
Inductor	Newport 1 410 454	100 μ H, 5.4 A, 46 m Ω
Input capacitor	Philips 136RVI	220 μ F, 35 V, 870 m Ω , 0.83 A
Output capacitor	Philips 136RVI	2 2200 μ F, 35 V, 100 m Ω , 2.6 A
MOSFET (upgraded)	IR IRFZ44N	55 V, 49 A, 22 m Ω
Inductor (upgraded)	Coilcraft PCV – 0 – 473 – 10	47 μ H, 10 A, 23 m Ω

	Buck	Boost	Buck – Boost	Cúk
Inductor(s)	100 μ H	100 μ H	2 100 μ H	2 100 μ H
Input cap	2 2200 μ F	220 μ F	2 2200 μ F	220 μ F
Output cap	220 μ F	2 2200 μ F	2 2200 μ F	220 μ F
Transfer cap				4 2200 μ F

Four 2200- μ F capacitors were specified for the Cúk converter transfer capacitor, and the buck-boost inductor was composed of two paralleled inductors shown in the equation at the top of the page.

Despite having about twice the volume of capacitors, and twice the volume of inductors, the buck-boost and Cúk converters fared badly compared to the other converters due to their high semiconductor conduction and switching losses (see Fig. 5, top). The buck converter bettered the boost, especially at lower currents, since a MOSFET rather than a Schottky diode is in the direct input-output path.

Two further simulations were completed with a goal of higher efficiency rather than lowest cost and simplicity. Firstly the MOSFETs were upgraded to IRFZ44N devices, with much lower on resistances, and another prewound inductor with half the series resistance and a higher saturation current was chosen. These changes made a large difference to all converters, especially at higher currents (see Fig. 5).

Secondly, the impact of a synchronous rectifier utilising a second IRFZ44N MOSFET was investigated. Switching speeds were also assumed improved from 150 to 100 ns total switching time per cycle, since these had become the largest single remaining loss.

The synchronous rectifier made a large difference to all converters except the buck converter (see Fig. 5, bottom). It may be unnecessary to introduce the extra complexity and cost of a synchronous rectifier and high side driver for the buck converter.

The final efficiency of the buck converter was over 96% over the range of 20–70 W. A loss of 3% at 60 W is less than 2 W. It is hoped that the potential gain in maximum power point tracking alone will more than compensate for this loss. Continuing research will examine an experimental string of dc–dc converters to determine if the predicted efficiencies can be obtained in practice. The control strategies of these distributed converters will also be examined.

VII. CONCLUSION

New residential scale photovoltaic (PV) arrays (<3 kW) are commonly connected to the grid by one of two approaches—a

single dc–ac inverter connected to a series string of PV panels, or many small dc–ac inverters which connect one or two panels directly to the ac grid. A “converter-per-panel” approach offers many advantages including

- 1) individual panel maximum power point tracking, which gives great flexibility in panel layout, replacement, and insensitivity to shading;
- 2) better protection of PV sources and redundancy in the case of source or converter failure;
- 3) easier and safer installation and maintenance;
- 4) better data gathering.

However, dc–ac per-panel inverters must step from a low dc voltage directly to a high ac voltage. Every panel must have an ac inverter and associated protection and filtering components. This imposes an efficiency and cost penalty on this approach.

Simple nonisolated per-panel dc–dc converters can be series connected to create a high voltage string connected to a single simplified dc–ac inverter. The advantages of per-panel converters are available without the cost or efficiency penalties.

Buck, boost, buck-boost, and Cúk converters are examined as possible cascaded converters. The boost converter is best if a significant step up is required, such as with a short string of 12-PV panels. However, under unusual unfavorable conditions, the boost converter string cannot always deliver all the power from a mixture of shaded panels and those delivering full power.

A string of buck converters requires many more panels, but can always deliver any combination of panel power. The buck converter will be the most efficient topology for a given cost.

While flexible in voltage ranges, buck-boost and Cúk converters are always at an efficiency or alternatively cost disadvantage.

APPENDIX EXAMPLE MATLAB SCRIPT

This Matlab script file (see Table I) is used to calculate the boost converter power loss components and overall power loss. The results are compared with experimentally gathered data.

REFERENCES

- [1] S. R. Wenham, M. A. Green, and M. Watt, *Applied Photovoltaics*. Sydney, Australia: Univ. New South Wales, 1994.
- [2] J. Larminie and A. Dicks, *Fuel Cell Systems Explained*. New York: Wiley, 2000.
- [3] D. A. J. Rand, R. Woods, and R. M. Dell, *Batteries for Electric Vehicles*. New York: Wiley, 1998.
- [4] M. Calais, J. M. A. Myrzik, and V. G. Agelidis, "Inverters for single phase grid connected photovoltaic systems—overview and prospects," in *Proc. 17th PV Solar Energy Conf. and Exhibition*, Munich, Germany, Oct. 2001.
- [5] T. Noguchi, S. Togashi, and R. Nakamoto, "Short-circuit pulse-based maximum-power-point tracking method for multiple photovoltaic-and-converter module system," *IEEE Trans. Ind. Electron.*, vol. 49, pp. 217–223, Feb. 2002.
- [6] L. M. Tolbert and F. Z. Peng, "Multilevel converters as a utility interface for renewable energy systems," in *IEEE PES Summer Meeting*, Seattle, WA, 2000.
- [7] M. Calais and V. G. Agelidis, "Multilevel converters for single-phase grid connected photovoltaic systems-an overview," in *Proc. IEEE International Symp. Industrial Electronics*, Pretoria, South Africa, 1998.
- [8] J. H. R. Enslin, M. S. Wolf, D. B. Snyman, and W. Swiegers, "Integrated photovoltaic maximum power point tracking converter," *IEEE Trans. Ind. Electron.*, vol. 44, pp. 769–773, Dec. 1997.
- [9] R. Giri, R. Ayyana, and N. Mohan, "Common duty ratio control of input series connected modular dc-dc converters with active input voltage and load current sharing," in *Proc. 18th Annu. IEEE Applied Power Electronics Conf. Expo. (APEC'03)*, vol. 1, Feb. 2003, pp. 322–326.
- [10] G. Walker, "Evaluating MPPT converter topologies using a MATLAB PV model," *J. Elect. Electron. Eng. Australia*, vol. 21, pp. 49–56, 2001.
- [11] F. Hamma, T. Meynard, F. Tourkhani, and P. Viarouge, "Characteristics and design of multilevel choppers," in *Power Electronics Specialists Conf. (PESC'95)*, vol. 2, 1995, pp. 1208–1214.
- [12] N. Mohan, T. M. Undeland, and W. P. Robbins, *Power Electronics: Converters, Applications, and Design*, 2nd ed. New York: Wiley, 1995.
- [13] BP Solar. (2003, Dec.) BP SX 60 Datasheet. Tech. Rep., BP Solar. [Online] Available: <http://www.bpsolar.com/>



Geoffrey R. Walker (M'99) was born in Brisbane, Australia, in 1969. He received the B.E. degree and the Ph.D. degree in multilevel converter modulation and control from The University of Queensland, St. Lucia, Australia, in 1990 and 1999, respectively.

He is currently a Lecturer in the School of Information Technology and Electrical Engineering (ITEE), and Researcher in the Sustainable Energy Research Group (SERG), The University of Queensland. He has worked in both the professional audio and industrial electronics industries, performing both design

and repair work, and continues to consult in these fields. His interests are in the areas of electronics, power electronics, and electric machines, as they are applied to sustainable energy production and use.



Paul C. Sernia was born in Melbourne, Australia, in 1978. He received the B.E and B.Sc degrees from the University of Queensland, Australia, in 2000 where he is currently pursuing the Ph.D. degree in the School of Information Technology and Electrical Engineering (ITEE).

His current research is in the effects of random modulation in multilevel converters. His other interests lie in the fields of power electronics for vehicle and renewable energy applications.